IEEE Photonics Journal
An IEEE Photonics Society Publication

Open Access

A Novel Method for Constructing VLC Equalizer With Active-Passive Hybrid Network

Volume 12, Number 1, February 2020

Chengyu Min
Xiongbin Chen
Xurui Mao
Xuanjie Li
Tianhao Pan
Qigong Sun
Hongda Chen

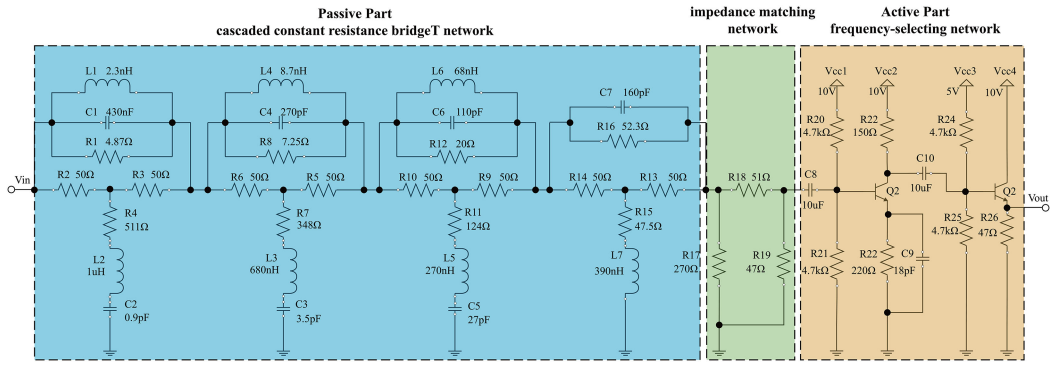

DOI: 10.1109/JPHOT.2020.2969413

A Novel Method for Constructing VLC Equalizer With Active-Passive Hybrid Network

Chengyu Min,[1] **Xiongbin Chen**,[1,2,3] **Xurui Mao**,[1] **Xuanjie Li**,[2] **Tianhao Pan**,[3] **Qigong Sun**,[1] **and Hongda Chen**[1]

[1] State Key Laboratory on Integrated Optoelectronics, Institute of Semiconductors, Chinese Academy of Sciences, Beijing 100083, China
[2] School of Electronic, Electrical and Communication Engineering, University of Chinese Academy of Sciences, Beijing 101408, China
[3] Center of Materials Science and Optoelectronics Engineering, University of Chinese Academy of Sciences, Beijing 100049, China

DOI:10.1109/JPHOT.2020.2969413

Manuscript received November 28, 2019; revised January 7, 2020; accepted January 21, 2020. Date of publication January 27, 2020; date of current version March 19, 2020. This work was supported in part by the National Key R&D Program of China under Grant 2017YFB0403604, in part by the National Natural Science Foundation of China under Grant 61875183, in part by the High Tech Youth Talent Program of the Chinese Academy of Sciences under Grant GQRC-19-03. Corresponding author: Chengyu Min (e-mail: minchengyu@semi.ac.cn).

Abstract: In this article, a novel method for constructing a pre-equalizer by optimized filter synthesis with vector fitting is proposed to broaden the bandwidth of a visible light communication (VLC) system. By using the proposed method, an active-passive hybrid equalization circuit is constructed, and it is demonstrated that the 3-dB bandwidth of the VLC system with commercially available phosphorescent white LED is extended from 30 MHz to 600 MHz. A 1.35 Gb/s NRZ-OOK VLC transmission over 12 cm free space transmission distance is experimentally realized, achieving a bit error rate (BER) of 8.8×10^{-5}. To the best of the authors knowledge, this is the largest reported 3-dB bandwidth and real-time data rate achieved in the VLC system with a single commercially phosphorescent white LED.

Index Terms: VLC, pre-equalization circuit, vector fitting, filter synthesis, bridge-T structure.

1. Introduction

The light-emitting diodes (LEDs) have been considered to be the most promising devices for the next-generation illumination, due to their advantages of energy-saving, lifespan advantages, and compact form factor [1]. It has been expected that by 2030, the LED will provide about 75% of all the illumination, which will provide a unique opportunity for visible light communications (VLC) based on LEDs [2]. The LEDs are capable of fast switching to different light intensity levels, which can be used to transmit the data encoded in the emitting light in various ways [3], [4].

However, the limited bandwidth of commercial LEDs prevents VLC systems from achieving high-speed transmission [5]. Recently, several technologies have been proposed to extend the 3-dB bandwidth, such as using the analogy pre- and post-equalization technology, blue light filtering and software pre-equalization or pre-emphasis scheme. Software equalization can provide more

accurate equalization compared to hardware equalization [6]. Meanwhile software equalization needs a lot of computational resources which may decrease the data rate when the training sequences are too many [7]. On the other hand, hardware equalization is designed to achieve transparent transmission. So, hardware equalization can provide a stable bandwidth compensation without occupying computational resources. Therefore, the comprehensive utilization of software equalization and hardware equalization can reduce system complexity and improve system performance. Especially in [8], Zhou *et al.* experimentally demonstrated a 15 Gb/s underwater VLC transmission employing hardware equalization and software equalization simultaneously. In 2008, Le-Minh first proposed a pre-equalization circuit that increased the 3-dB bandwidth to 45 MHz and realized an 80 Mb/s Non-Return to Zero On-Off Keying (NRZ-OOK) data transmission [9]. In 2014, Li achieved a 550 Mb/s real-time NRZ-OOK data transmission using a phosphorescent white LED. By utilizing the pre-emphasis, post-equalization circuits, and a blue filter, the 3-dB bandwidth of the VLC system was extended to 233 MHz [10]. In 2015, using a cascaded bridged-T equalizer circuit and a blue filter, Huang increased the 3-dB bandwidth to 366 MHz and realized a 1.6 Gbit/s offline VLC transmission using the quadrature amplitude modulation with orthogonal frequency division multiplexing (16QAM-OFDM) [11]. In 2018, Zhang used a bridged-T cascaded pre-equalization circuit to extend the 3-dB bandwidth of the VLC system from 1 MHz to 520 MHz, which has been the highest reported 3-dB bandwidth of VLC system based on phosphorescent white LED. By using the pre-equalization circuit, a 1 Gb/s data rate VLC system was realized [12].

Hitherto, the research on equalization circuits has been mainly based on experiments with a certain circuit having appropriate parameters. However, the characteristics of an LED and VLC system components vary among different models. Therefore, we propose a top-down method to design an ideal equalizer. The proposed method has great universality and can be applied to the most VLC systems. First, the equalization transfer function is calculated from the vector fitting result of an LED. Then, an all-pass function is used to move the poles of the transfer function, making the processed equalization transfer function physically achievable. Finally, an active-passive hybrid equalization circuit is constructed by the optimized filter synthesis.

By employing the proposed method, an active-passive hybrid pre-equalization circuit is designed to evaluate the 3-dB bandwidth of a VLC system, and it is found that the 3-dB bandwidth is improved from 30 MHz to 600 MHz using a single commercially available phosphorescent white LED. Moreover, it is demonstrated experimentally that a 1.35 Gb/s real-time NRZ-OOK VLC system over a 12 cm free space transmission distance achieves a bit error rate (BER) of 8.8×10^{-5}, which is below the forward error correction (FEC) limit of 3.8×10^{-3}. To the best of authors knowledge, these have been the highest data rate, and the widest 3-dB bandwidth ever achieved utilizing a commercially available phosphorescent white LED in a real-time NRZ-OOK VLC system.

The contributions of this paper are as follows.

- A novel active-passive hybrid equalization method is developed using the vector fitting result of an LED. The proposed method enables a change in the equalization circuit structure with the change in the system characteristics, resulting in better system adaptability.
- The vector fitting algorithm is optimized for obtaining an accurate and physically achievable equalization transfer function by adding a specific all-pass network processing.
- It is proposed to group the equalization zeros and poles, and then to construct the equalization by using a bridge T-type network according to the certain group, thus making the equalization circuit easy to construct by using high-order rational function approximations.
- An active-passive hybrid equalization circuit is proposed to avoid receiver sensitivity decreasing in a passive equalizer.
- The proposed method is verified experimentally with a 1.35 Gb/s phosphorescent white LED NRZ-OOK real-time VLC transmission, achieving a BER of 8.8×10^{-5}, which is below the FEC limit of 3.8×10^{-3}. The 3-dB bandwidth of the system is extended from 30 MHz to 600 MHz using a blue filter.

2. Proposed Method

This section presents the proposed method. First, the rational approximation of the frequency response optimized by vector fitting is introduced in Section 2.1. The vector fitting result is used to calculate the equalization transfer function using a specific all-pass function. Then, in Section 2.2, it is explained how to construct an active-passive hybrid equalization circuit using an optimized filter synthesis.

2.1 Rational Approximation of the Frequency Response of an LED Optimized by Vector Fitting

With the aim to obtain an accurate equalization transfer function, the frequency response of an LED has to be measured and replaced with the rational function approximation. A rational function approximation of a given N^{th} order can be expressed as [13]:

$$f(s) \approx \frac{a_0 + a_1\, s + a_2\, s^2 + \cdots + a_N\, s^N}{b_0 + b_1\, s + b_2\, s^2 + \cdots + b_N\, s^N} \tag{1}$$

In this work, the vector fitting algorithm presented in [14] is used. In this subsection, it is explained how to optimize the vector fitting algorithm for the purpose of achieving an accurate and physically achievable equalization transfer function. The vector fitting algorithm is briefly described in the following. The rational approximation of the frequency response of an LED is calculated using the vector fitting method, which includes two steps. In the first stage, a set of starting poles is obtained by:

$$f(s) \approx \sum_{n=1}^{N} \frac{c_n}{s - a_n} + d \tag{2}$$

where a_n denotes the pole of the rational function $f(s)$, and c_n denotes the residue corresponding to pole a_n; d is a polynomial of s; s is the complex parameter in the Laplace transform. According to the vector fitting result of an LED, d is a constant term. It is worth noting that a residue c_n and a pole a_n are either real or complex conjugate pairs. Then, an unknown function σ(s) with rational approximation is introduced. As given by (3), $f(s)$ is multiplied by σ(s), and it is assumed that σ(s) has the same poles as $\sigma(s) \times f(s)$.

$$\begin{bmatrix} \sigma(s) f(s) \\ \sigma(s) \end{bmatrix} \approx \begin{bmatrix} \sum_{n=1}^{N} \frac{c_n}{s - \bar{a}_n} + d \\ \sum_{n=1}^{N} \frac{\tilde{c}_n}{s - \bar{a}_n} + 1 \end{bmatrix} \tag{3}$$

By multiplying the second row in (3) with $f(s)$, we can get (4) and (5).

$$\left(\sum_{n=1}^{N} \frac{c_n}{s - \bar{a}_n} + d \right) = \left(\sum_{n=1}^{N} \frac{\tilde{c}_n}{s - \bar{a}_n} + 1 \right) f(s) \tag{4}$$

$$(\sigma f)_{fit}(s) = \sigma_{fit}(s) f(s) \tag{5}$$

Then, $f(s)$ can be obtained by solving (4) like an overdetermined linear problem. Also, (5) can be transformed into the transfer function given by:

$$(\sigma f)_{fit}(s) = h \frac{\prod_{n=1}^{N+1} (s - z_n)}{\prod_{n=1}^{N} (s - \bar{a}_n)} \quad , \quad \sigma_{fit}(s) = \frac{\prod_{n=1}^{N} (s - \tilde{z}_n)}{\prod_{n=1}^{N} (s - \bar{a}_n)} \tag{6}$$

Combining (5) and (6), we get:

$$f(s) = \frac{(\sigma f)_{fit}(s)}{\sigma_{fit}(s)} = h \frac{\prod_{n=1}^{N+1} (s - z_n)}{\prod_{n=1}^{N} (s - \tilde{z}_n)} \tag{7}$$

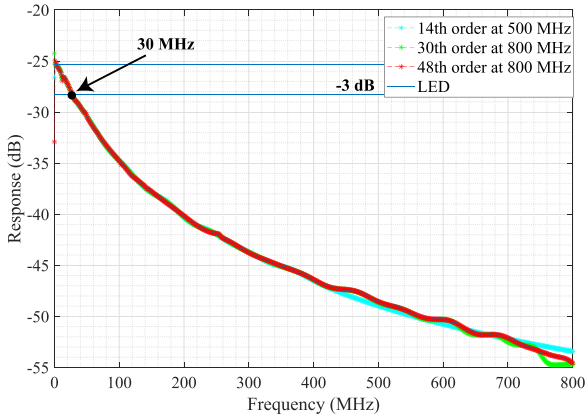

Fig. 1. The vector fitting curve at different order of rational function.

Notice that poles of function $f(s)$ are the same as zeros of function σ_{fit}(s) in (7). Therefore, we can obtain a set of poles of function $f(s)$ by calculating zeros of function σ_{fit}(s).

In the second stage, the obtained zeros of σ_{fit}(s) are set as new poles of $f(s)$, and the first stage is repeated. After several iterations, zeros of function σ_{fit}(s) converge toward the ideal poles of function $f(s)$.

Once the final poles of function $f(s)$ are obtained, the residues of function $f(s)$ can be calculated by (7).

We performed vector fitting on the frequency response of an LED in different frequency ranges with different order of rational function. The results of vector fitting are shown in Fig. 1.

As shown in Fig. 1, the order of rational function affects the accuracy of vector fitting. With the order of rational function increases, the vector fitting becomes more accurate is, but the circuit becomes more complex. Thus, it is needed to balance the accuracy with the circuit complexity according to certain requirements. Furthermore, due to the bandwidth limitation of an LED, a high-frequency signal is subjected to noise interference, so only the frequency response of an LED is fitted before 500 MHz, as shown in Fig. 1. Since it holds that $f(s) \times H_{ideal}(s) = 1$, the ideal equalization transfer function $H_{ideal}(s)$ is a reciprocal of function $f(s)$. However, as shown in Fig. 2, the poles of function $H_{ideal}(s)$ are distributed in the right half of the pole-zero plot, which makes the circuit constructed by $H_{ideal}(s)$ oscillate.

Therefore, we propose to add a specific all-pass filter $H_{allpass}(s)$ to move the poles of function $H_{ideal}(s)$ to the left half of the pole-zero plot. The zeros of the all-pass filter have the same position as the poles of function $H_{ideal}(s)$. As a result, function $H_{feasible}(s)$ has the same poles as function $H_{allpass}(s)$, and the same zeros as function $H_{ideal}(s)$, which is given by:

$$H_{feasible}(s) = H_{ideal}(s) \times H_{allpass}(s) \tag{8}$$

It is worth noting that the all-pass filter has no effect on the frequency response of function $H_{ideal}(s)$. Therefore, the frequency response of function $H_{feasible}(s)$ is the same as the frequency response of function $H_{ideal}(s)$, as shown in Fig. 3.

Thus, the poles of function $H_{feasible}(s)$ are distributed in the left half of the pole-zero plot; thus, the transfer function $H_{feasible}(s)$ can be used to construct the ideal equalization circuit.

2.2 Construct Equalization Circuit by the Optimized Filter Synthesis

As shown in Fig. 3, the frequency response curve of the ideal equalizer increases monotonously with the frequency. However, the filter synthesis method uses pure passive components to establish the circuit, which cannot provide sufficient signal gain. Hence, the filter synthesis method cannot

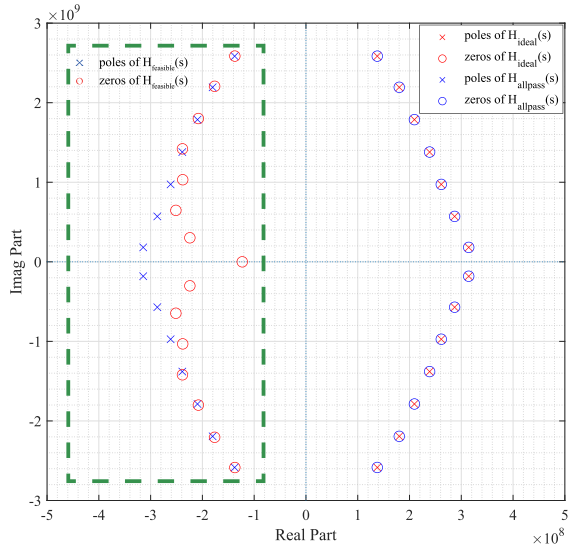

Fig. 2. The zero-pole plots of functions $H_{ideal}(s)$, $H_{allpass}(s)$ and $H_{feasible}(s)$.

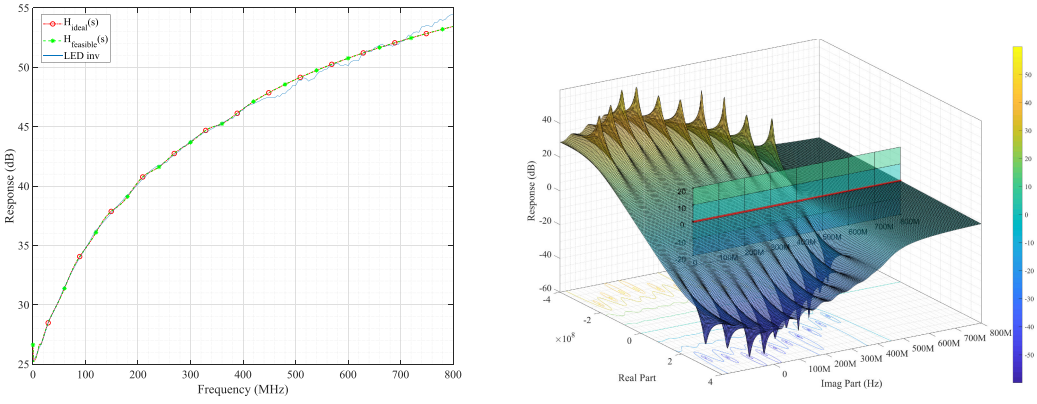

(a) (b)

Fig. 3. (a) Frequency response of functions $H_{ideal}(s)$, $H_{feasible}(s)$ and inverse frequency response of LED. (b) The zero-pole and frequency response of $H_{allpass}(s)$.

be utilized to construct the circuit represented by $H_{feasible}(s)$. In order to overcome this problem, we propose adding a pole into $H_{feasible}(s)$, and then offsetting the pole by adding an active RC circuit after $H_{feasible}(s)$ as follows:

$$H_{RC}(s) = a_{RC}\,(s - z_{RC}) \tag{9}$$

$$H_{passive}(s) = \frac{H_{feasible}(s)}{a_{RC}\,(s - z_{RC})} \tag{10}$$

$$H_{feasible}(s) = H_{passive}(s) \times H_{RC}(s) \tag{11}$$

where function $H_{RC}(s)$ denotes the transfer function of the active RC circuit, and function $H_{passive}(s)$ denotes the transfer function of the passive part of an equalizer. It can be found that the transfer function of $H_{feasible}(s) \times H_{RC}(s)$ is the same as the transfer function of $H_{feasible}(s)$, which means an equalizer can be composed of a passive circuit defined by $H_{passive}(s)$ and an active RC circuit defined by $H_{RC}(s)$. Considering the limitation of the gain-bandwidth product, we select a transistor to realize

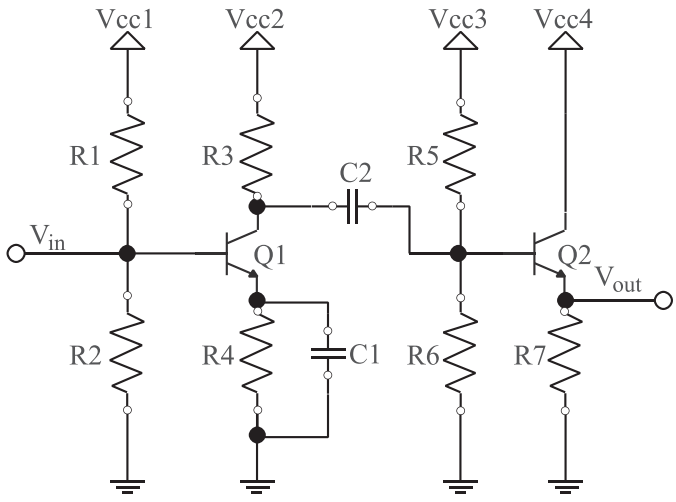

Fig. 4. An active RC circuit.

an active RC circuit. As shown in Fig. 4, a frequency-selecting network and an emitter follower are connected by a blocking capacitor C2.

In the frequency-selecting network, resistors R1 and R2 are used as bias resistors to set the static operating point of transistor Q1. Resistors R3 and R4 and capacitor C1 are used to enable a single-pole amplification network, as given by:

$$H_{RC}(s) = \frac{R_3}{R_4//(1/sC_1)} = R_3 \times C_1 \times \left(s + \left(\frac{R_4}{R_3^2 \times C_1}\right)\right) \tag{12}$$

The emitter follower is used as a stage isolator, and resistors R5 and R6 are used as bias resistors to set the static operating point of transistor Q2; lastly, resistor R7 is used to convert the current signal into a voltage signal.

After adding the pole of active RC circuit into $H_{feasible}(s)$, the highest order of numerator polynomial becomes the same as the highest order of the denominator polynomial of $H_{passive}(s)$. Thus, $H_{passive}(s)$ meets the requirements of the filter synthesis method for circuit constructing. However, the high order of rational approximation used to fit the curve accurately makes the Ladder network construction quite difficult in terms of filter synthesis. Conventional continued fraction approximation is also limited because the poles and zeros of $H_{passive}(s)$ are not on the imag axis. In order to solve this problem, we propose grouping adjacent poles and zeros of $H_{passive}(s)$ to split the high-order transfer function into multiple low-order transfer functions, which is given by:

$$H_{passive}(s) = \frac{(s-z_1)(s-z_2)\ldots(s-z_{n-1})(s-z_n)}{(s-p_1)(s-p_2)\ldots(s-p_{n-1})(s-p_n)} = \frac{(s-z_1)(s-z_2)}{(s-p_1)(s-p_2)} \times \cdots \times \frac{(s-z_{n-1})(s-z_n)}{(s-p_{n-1})(s-p_n)} \tag{13}$$

According to the vector fitting, z_n denotes the zero of function $H_{passive}(s)$, p_n denotes the pole of function $H_{passive}(s)$. z_1 and z_2, p_1 and p_2 are respectively conjugated. As given by (13), for each low-order transfer function, the corresponding circuit can be constructed by filter synthesis. Nonetheless, due to the impedance matching problem, transfer function of cascaded circuit is different from $H_{passive}(s)$. With the aim to overcome this problem, we introduce a cascaded constant-resistance bridged-T network to implement the multiple low-order transfer functions [13], as shown in Fig. 5.

V_{in} denotes the input signal of this bridge-T network. V_{out} denotes the output signal of this bridge-T network. Z_{11} and Z_{21} respectively represent the impedances in a set of inverse networks. c denotes an arbitrary real. When $Z_{11}Z_{21} = R^2$ and $c \geq 1$, the input impedance and output impedance are

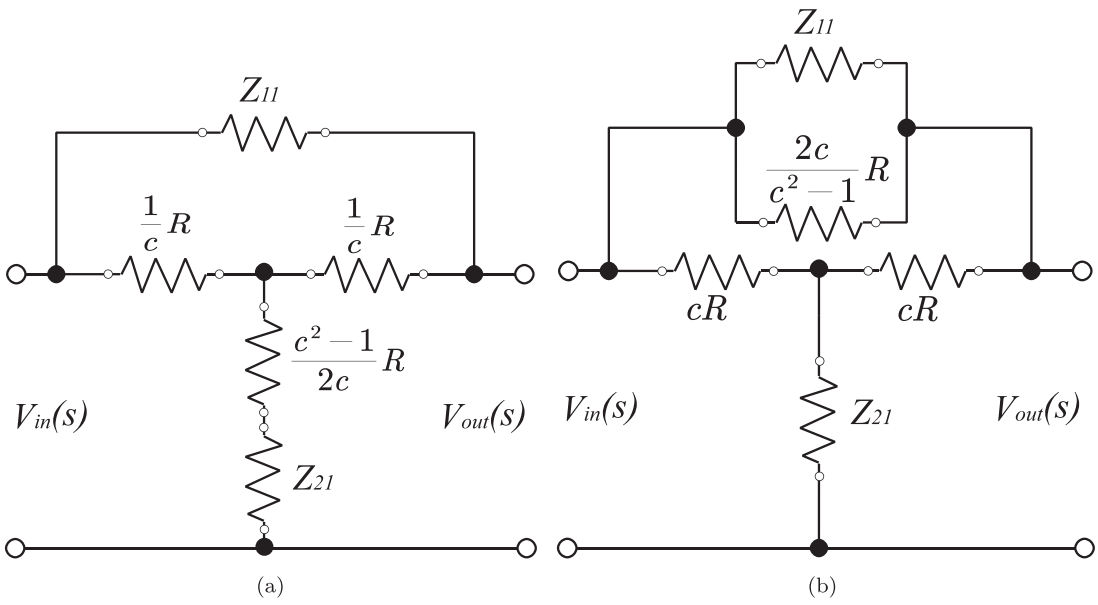

Fig. 5. Two types of a constant-resistance bridged-T network.

both constant and equal to R. Then, the transfer voltage ratio of the constant-resistance bridged-T network is given by (14), and at c = 1, it can be rewritten by (15).

$$\frac{V_{in}(s)}{V_{out}(s)} = \frac{1 + (c+1)\,Z_{11}/2R}{1 + (c-1)\,Z_{11}/2R} \tag{14}$$

$$\frac{V_{in}(s)}{V_{out}(s)} = 1 + Z_{11}/R \tag{15}$$

Combining the transfer function $H_{bridgeT}(s) = V_{out}(s)/V_{in}(s)$ and (15), we can get:

$$H_{bridgeT}(s) = \frac{1}{1 + Z_{11}/R} \tag{16}$$

Due to the constant input and output impedances of the bridged-T network, we can construct the corresponding circuit for each low-order transfer function by Z_{11}.

An active-passive hybrid equalization circuit is constructed to verify the above-presented method based on the frequency response of a commercial white phosphorescent LED with a blue filter.

As shown in Fig. 6, the equalization circuit is composed of a cascaded passive constant resistance bridged-T network, an impedance matching network, and an active RC frequency-selecting network.

The parameters of resistors, capacitors, and inductors in the equalization circuit are not exactly the same as their deduced values because, for some of the deduced values, there have not been the corresponding components.

3. Experimental Verification

3.1 Bandwidth Measurement Experiment and Results

The block diagram and experimental setup of the VLC system are presented in Fig. 7.

First, the frequency response of the VLC system was measured, and the measurement result is shown in Fig. 7. At the transmitter side, the driving signal from Port1 of the vector network analyzer (VNA, Agilent, E5071B) was equalized by the active-passive hybrid equalizer. After being amplified

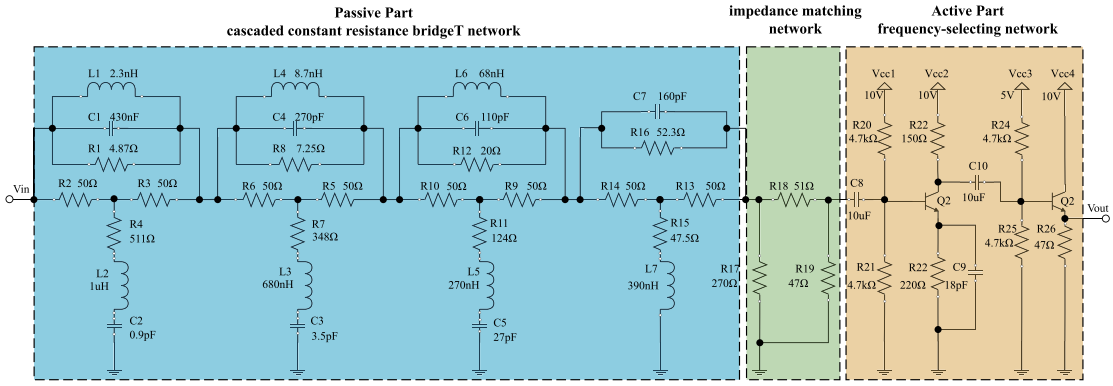

Fig. 6. Proposed equalization circuit consisting of passive part, impedance matching network, and active part.

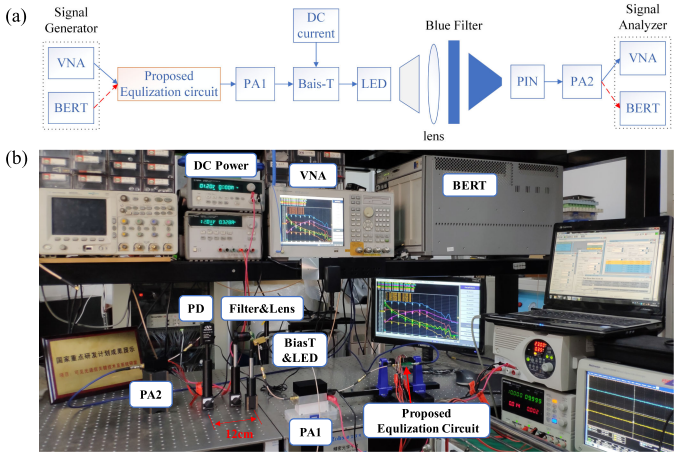

Fig. 7. (a) The block diagram of the constructed VLC system. (b) The VLC experimental setup.

by the power amplifier PA1 (RF-BAY, MPA-10-40, 1 MHz-1000 MHz bandwidth), the resulting signal was coupled with direct current (DC) of 350 mA by the bias tee (INMET, 8810 s, 50 kHz-18 GHz bandwidth). After that, the signal was applied to a commercial phosphorescent white LED (OSRAM, LUW-CN7N, 150 lm at 350 mA). A lens was fixed in front of the LED at an appropriate distance to focus the light in order to improve the signal-to-noise ratio (SNR) of the system. At the receiver side, a blue filter was placed in front of an amplified silicon PIN detector (Newport, 818-BB-21 A, 30 kHz-1.2 GHz bandwidth) to remove the slow-responding phosphor component. The distance between the LED and the PIN detector was 12 cm. Another power amplifier PA2 (ixblue, DR-AN-20-MO, 50 kHz-20 GHz bandwidth) was used to amplify the photocurrent output signal of the PIN detector. Finally, the output signal of the PA2 was fed to Port2 of the VNA. By using the VLC experimental setup presented in Fig. 7, we measured the frequency response of the VLC system with the equalization circuit. The frequency responses of the LED, equalizer, and the VLC link with equalizer are displayed in Fig. 8.

In order to facilitate the analysis of the obtained experimental results, we added the inverse frequency response of the LED in Fig. 8, which denoted the frequency response of the ideal equalizer.

As shown in Fig. 8, the frequency response of the proposed equalizer was in agreement with the frequency response of the ideal equalizer in the frequency range from 1 MHz to 500 MHz. The frequency response of the proposed equalizer was limited by the gain-bandwidth product

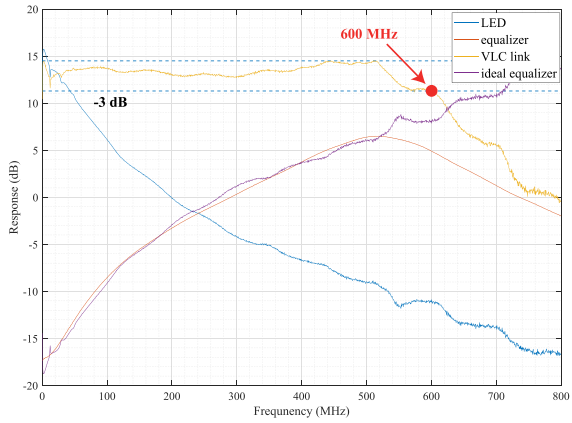

Fig. 8. The measured frequency responses of LED, equalizer, VLC link, and ideal equalizer.

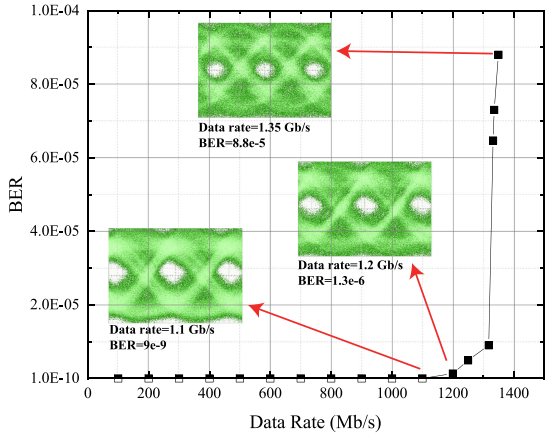

Fig. 9. The measured BER at different data rate and eye diagrams.

of the transistor, so the response started to decrease after the frequency of 500 MHz, while the frequency response of the LED decreased slowly in the frequency range from 500 MHz to 600 MHz. Therefore, the 3-dB bandwidth of the phosphorescent LED-based VLC link was improved to 600 MHz. Thus, the 3-dB bandwidth of the VLC link was from 1 MHz to 600 MHz, which ensured that the SNR in a low-frequency range would not be too low so that a good communication performance can be achieved.

3.2 Data Transmission Experiment and Results

In this experiment, the VLC experimental link presented in Fig. 7 was used to measure the BER of the VLC at a different data rate. At the transmitter side, the PRBS-7 (pseudo-random binary sequence in $2^7 - 1$) NRZ-OOK signal with a peak-to-peak voltage swing of 100 mV, generated by the BERT (Agilent, 81250) was fed to the proposed equalizer as an input of the phosphorescent LED-based VLC system. At the receiver side, the amplified photocurrent signal was fed to the BRET RX port as an input signal. In the experiment, different bit error rates were obtained at different input signal data rates; the input signal data rate was changed from 100 Mb/s to 1.35 Gb/s. The measured BER of the VLC link with the proposed equalizer is shown in Fig. 9.

At the BER of 8.8×10^{-5}, the highest data rate of the phosphorescent LED-based VLC link was 1350 Mb/s, which denotes the highest reported real-time data rate of a VLC system using a phosphorescent LED based on the NRZ-OOK modulation with the 3-dB bandwidth of 600 MHz.

Meanwhile, the BER of the VLC experimental link was measured for two hours at the data rate of 1.35 Gb/s to evaluate the stability of the constructed system. The experimental results verified the proposed method. Namely, the proposed equalizer significantly improved the 3-dB bandwidth and provided a high-speed real-time data transmission in the VLC link.

The limiting factors of the conducted experiment were the receiver signal amplitude and transmission channel noise. The photosensitivity of photodiode in the wavelength range from 400 nm to 500 nm was below 0.2 A/W, which made the weak optical signal amplitude decreased after being converted into photocurrent. Further, the weak photocurrent signal reduced the SNR, making the signal recovery difficult.

4. Conclusion

In this paper, a novel method for constructing the VLC equalizer with an active-passive hybrid network is proposed. The proposed method is verified experimentally by an active-passive hybrid equalizer using real-time phosphorescent white LED NRZ-OOK VLC transmission. The experimental results showed that the 3-dB bandwidth of the VLC link with a blue filter was extended from 30 MHz to 600 MHz. The highest real-time data rate of 1.35 Gb/s was achieved at the BER of 8.8×10^{-5}, which was below the forward error correction limit of 3.8×10^{-3}. To the authors best knowledge, this is the highest data rate and the widest 3-dB bandwidth ever reported in a real-time NRZ-OOK VLC system based on a single commercially available phosphorescent white LED in the VLC systems.

In the future, we plan to optimize the optical path design to increase the SNR in long-distance transmission. Also, we intend to apply other modulation schemes, such as DCO-OFDM, to improve the data rate further.

References

[1] H. P. Parth, F. Xiaotao, H. Pengfei, and M. Prasant, "Visible light communication, networking, and sensing: A survey, potential and challenges," *IEEE Commun. Surv. Tut.*, vol. 17, no. 4, pp. 2047–2077, Oct./Dec. 2015.
[2] J. Penning, K. Stober, V. Taylor, and M. Yamada, "Energy savings forecast of solid-state lighting in general illumination applications," Washington, DC, US: Navigant Consulting, Inc., Tech. Rep. DOE/EE-1467 7703, 2014.
[3] Y. Tanaka, S. Haruyama, and M. Nakagawa, "Wireless optical transmissions with white colored led for wireless home links," in *Proc. 11th IEEE Int. Symp. Personal Indoor Mobile Radio Commun. PIMRC 2000. Proc. (Cat. no. 00TH8525)*, London, U.K., vol. 2, Sep. 2000, pp. 1325–1329.
[4] T. Komine and M. Nakagawa, "Fundamental analysis for visible light communication system using led light," *IEEE Trans. Consum. Electron.*, vol. 50, no. 1, pp. 100–107, Feb. 2004.
[5] D. Karunatilaka, F. Zafar, V. Kalavally, and R. Parthiban, "Led based indoor visible light communications: State of the art," *IEEE Commun. Surv. Tut.*, vol. 17, no. 3, pp. 1–30, Jul.–Sep. 2015.
[6] Y. Zhou, J. Zhao, M. Zhang, J. Shi, and N. Chi, "2.32 gbit/s phosphorescent white led visible light communication aided by two-staged linear software equalizer," in *Proc. IEEE 10th Int. Symp. Commun. Syst., Netw. Digit. Signal Process.*, 2016, pp. 1–4.
[7] H. Qian, S. Yao, S. Cai, and T. Zhou, "Adaptive postdistortion for nonlinear leds in visible light communications," *IEEE Photon. J.*, vol. 6, no. 4, pp. 1–8, Aug. 2014.
[8] Y. Zhou *et al.*, "Common-anode led on a si substrate for beyond 15 gbit/s underwater visible light communication," *Photon. Res.*, vol. 7, no. 9, pp. 1019–1029, 2019.
[9] H. L. Minh *et al.*, "80 mbit/s visible light communications using pre-equalized white led," in *Proc. 34th Eur. Conf. Opt. Commun.*, 2008, pp. 1–2.
[10] H. Li, X. Chen, J. Guo, and H. Chen, "A 550 mbit/s real-time visible light communication system based on phosphorescent white light led for practical high-speed low-complexity application," *Opt. Express*, vol. 22, no. 22, pp. 27 203–13, 2014.
[11] X. Huang, Z. Wang, J. Shi, Y. Wang, and N. Chi, "1.6 gbit/s phosphorescent white led based vlc transmission using a cascaded pre-equalization circuit and a differential outputs pin receiver," *Opt. Express*, vol. 23, no. 17, 2015, Art. no. 22034.
[12] H. Zhang, A. Yang, L. Feng, and P. Guo, "Gb/s real-time visible light communication system based on white leds using t-bridge cascaded pre-equalization circuit," *IEEE Photon. J.*, vol. 10, no. 2, Apr. 2016, Art. no. 7901807.
[13] O. J. Zobel, "Distortion correction in electrical circuits with constant resistance recurrent networks," vol. 7, no. 3, pp. 438–534, 2013.
[14] B. Gustavsen and A. Semlyen, "Rational approximation of frequency domain responses by vector fIltIng," *IEEE Trans. Power Del.*, vol. 14, no. 3, pp. 1052–1061, Jul. 1999.